ANDRZEJ GAJEK[*)]

EVALUATION OF ABS OPERATION ON DRUM STAND

The paper presents the results of simulation and research of antilock braking systems (ABS) carried out on the fast rotating drum stand with flywheels. The model of the vehicle–drum stand system was presented. The influence of car suspension and tyre parameters during braking with ABS on vehicle vibrations was analysed. Theoretical analyses of the simulations were verified during car tests on a prototype drum stand. The results of braking tests for passenger car on the homogeneous surface and on the surface with changed adhesion coefficient were presented. Qualitative criteria for diagnostic evaluation of ABS operation were proposed.

1. Introduction

So far, diagnostic control of ABS during exploitation has included only current examination of electronic and electrical parts. It has been realised by the selfmonitoring system integrated with the electronic control unit ECU and by diagnostic testers in stand conditions. This diagnostic system checks electronic and electrical elements. Mechanical and hydraulic parts are not controlled currently. Up to now, the routine, periodic vehicle brakes inspection does not include checking the ABS operation as a total unit, which would allow us to examine the effect of ABS operation (to check wheels speed and slip at time of braking). It is an important problem, because the interaction between electrical and mechanical parts decides of correct operation of ABS. The kinetic method of brakes control on the drum stand with flywheels gives the possibility to examine the ABS operation as a total unit. In the paper the author presents the construction of the stand, model of reaction between the vehicle and drum stand and the results of braking tests on homogeneous surface of the stand and on the surface with changed adhesion coefficient.

[*)]   *Cracow University of Technology, Institute of Automobiles, 31-864 Cracow, Al. Jana Pawła II 37; E-mail: gajeka@mech.pk.edu.pl*

2. Principle of stand control

Fig. 1 shows the scheme of the diagnostic stand. The tested car is driven on the four units of the stand. Each unit consists of driving drum 2 and support roller 1. Driving drums 2 are connected with flywheels 8 (front) or 9 (rear). Rear units can be shifted exactly to the wheel base of the tested car. Moments of inertia of the flywheels are divided into front and rear units in 2:1 ratio, corresponding to average brake distribution for passenger cars. Setting of drum 2 and support roller 1 (roller higher than drum) and direction of rotations
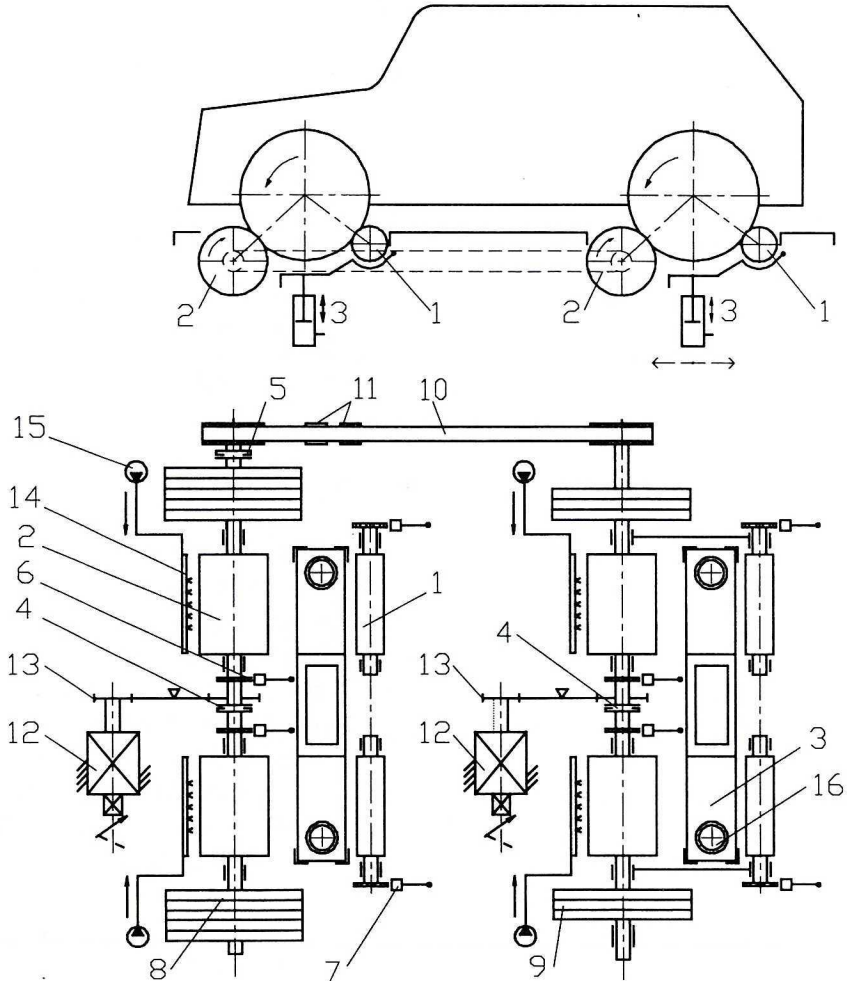

Fig. 1. Scheme of the test stand: 1 – support rollers, 2 – driving drums, 3 – system of car lifting and blocking support rollers, 4, 5 – electromagnetic clutches, 6,7 – drum and roller speed sensors, 8, 9 – flywheels for front and rear units, 10,11 – transmission (toothed belt and belt stretcher), 12 – electrical drive, 13 – transmission, 14 – sprayers, 15 – sprayer pumps, 16 – safety (stop) rollers

prevents the car wheels from being thrown out from the stand and keeps them in contact with rollers and drums. The stand is equipped with a system for lifting the car and blocking support rollers for safety of drive on and drive out from the stand (3 in Fig. 1). During the test the electromagnetic clutches and toothed belt connect four units into one set. There is a possibility to carry out the test on disconnected units.

Tests on the disconnected units were performed when we wanted to calculate the value of brake forces individually for each wheel. Two electric motors gave the possibility to drive front or rear units individually.

Car wheels with driving drums, flywheels and support rollers were driven by electric motors 12. When the speed of the car wheels was about 45 ... 50 km/h, the electric drive was disconnected and the brakes were intensively used. Car wheels and rotating elements of the stand were braked until they stand still. During braking, the ABS system started working. The peripheral speed of the drums 2 (it matched the speed of the car) and peripheral speed of the rollers 1 (as the speed of the braked wheels) were measured. The digital sensors (1000 imp./rev.) were used. The measured parameters were automatically transferred to a computer.

The investigation showed that, because of small mass of the roller 1 and its moment of inertia over ten times smaller than the car wheel, the slip between wheel and support roller was near zero. It made it possible (for diagnostic purposes) to calculate the speed of the car wheel on the basis of measurement of the velocity of the support roller.

The surface of support rollers ought to be coated with special material which has high adhesion coefficient when dry and wet. The stand makes it possible to change the tyre–drum coefficient of friction by electric sprayers 14. Spraying water on the individual drum surfaces allows for any combination of changes of the adhesion under the wheels (μ split and μ sprung surface). The stand makes it possible to test cars from 2.35m to 2.85m wheel base.

The investigation showed that the braked car maintained stability on the stand; there was no danger of throw out from the drums and there was no necessity for special holding of the car during the tests. The safety (stop) rollers 16 restricted the lateral displacement of the car on the stand. Bringing up to speed of about 50 km/h lasted about 2 min., time of the test was about 10 sec. The results of test (speeds, slips) were displayed graphically on the stand monitor directly after braking.

The diagnostic stand also allows testing systems preventing excessive wheel slip at time of acceleration (TCS systems).

3. Model of vehicle - drum stand system

Half vehicle model was used for analysis of braking on the stand. The model of the vehicle – drum stand consists of 6 rigid bodies connected by elastic and damping elements with linear characteristics (Fig. 2). The system has 12 degrees

of freedom: 3 – vehicle body (x, y – displacement, φ_N – rotation about y axis), 3 for front wheel, 3 for rear wheel (x, y, φ_k), 1 for each support roller 1 ($\varphi_{r1,p}$, $\varphi_{r1,t}$) and 1 for two drums with flywheels (φ_{r2}). The drums 2 are connected by toothed belt. The 1 degree of freedom for drums 2 means that toothed belt is longitudinally rigid. It was assumed that the vehicle did not move in the lateral direction. Only longitudinal and vertical vibrations and rotation about y axis were analysed. The damping and longitudinal/vertical stiffness of the front and rear suspension, as well as stiffness and damping of the tyre, were taken into account in the model. Influence of the tyre circumferential stiffness on the moment of rolling resistance of the wheel was taken into account in the model.
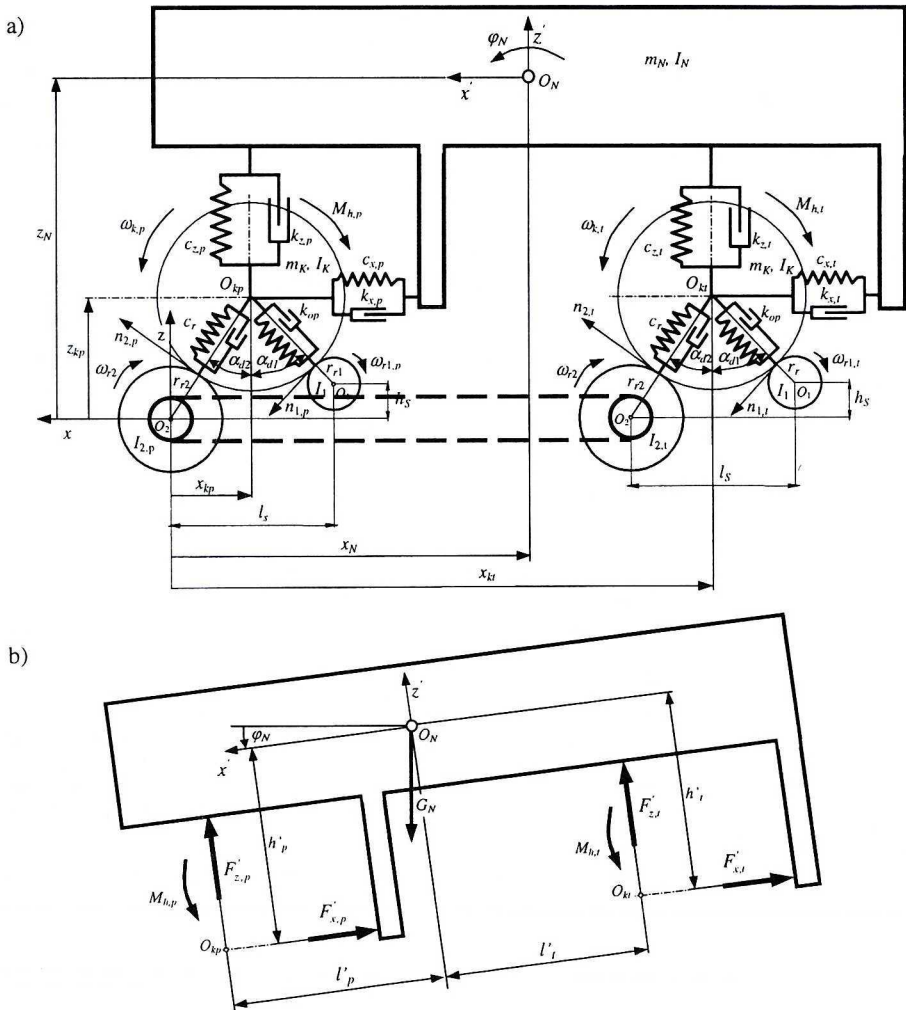

Fig. 2. Half vehicle model on the stand for ABS investigation. a) model of the vehicle – drum stand system, b) force system acting on the vehicle body, G_N – body weight, n_i – direction of F_{ni} force action

It was assumed that the lateral forces did not act on the wheels. Moments of inertia, longitudinal/vertical stiffness of the suspensions and tyres were determined experimentally for middle class passenger car. Rolling resistance of the wheels and drums were determined experimentally.

Preliminary tests showed that, during braking on the stand, the wheels displacement in relation to car body was small (about 0.01m). In that range of displacements, linear stiffness and damping characteristics of the suspension could be assumed.

It was assumed that mass, moments of inertia, stiffness and dumping of the front and rear wheels are equal: $m_{kp}=m_{kt}=m_k$, $I_{kp}=I_{kt}=I_k$, $c_{rp}=c_{rt}=c_r$, $k_{opp}=k_{opt}=k_{op}$.

The model of tyre presented in [7], [9] was used in the vehicle model. Some parameters of the tyre model were estimated on the basis of stand experiments.
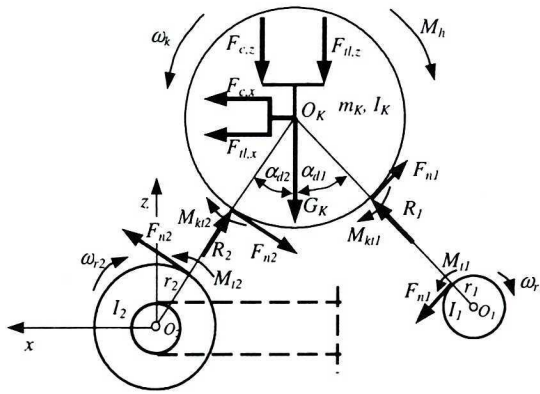

Fig. 3. Forces and moments acting on the wheel, drum and roller during braking on the stand. The resistance of wheel ventilation and resistance of bearings were neglected, G_k – wheel weight

Rill model of tyre [7], [9] allowed us to approximate the real characteristic of the tyre by function $F(F_z, s)$ in three intervals of the slip: $0 \leq s \leq s_M$, $s_M \leq s \leq s_S$, $s > s_S$ (Fig. 4). The lateral forces during braking on the stand were not analysed. The resultant tangential force F was the longitudinal force F_x (F_n force in the model of braking in Fig. 3). For the longitudinal force the tyre model was written as:

$$F_x(F_z,s)=\begin{cases} s_{xM}\left.\dfrac{dF_x}{ds_x}\right|_{s_x=0} \dfrac{\sigma}{1+\sigma\left[\left.\dfrac{s_{xM}}{F_{xM}}\dfrac{dF_x}{ds_x}\right|_{s=0}-2+\sigma\right]}, & \sigma=\dfrac{s_x}{s_{xM}}, 0\leq s_x \leq s_{xM}, \\[4ex] F_{xM}-(F_{xM}-F_{xs})\sigma^2(3-2\sigma), & \sigma=\dfrac{s_x-s_{xM}}{s_{xS}-s_{xM}}, s_{xM}\leq s_x \leq s_{xS}, \\[3ex] F_{xS} & s_x > s_{xS} \end{cases} \tag{1}$$
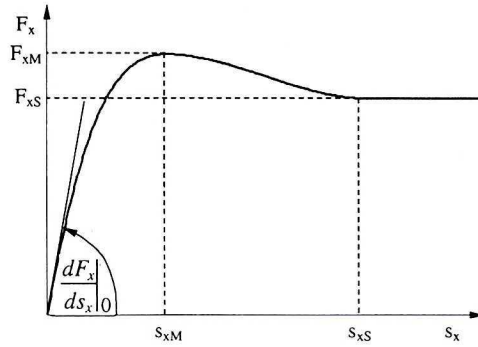
Fig. 4. Longitudinal force F_x versus longitudinal slip s_x

For determination of the F_x force, we need to establish five parameters (Fig. 4): slope dF_x/ds_x of the function $F_x(s_x)$ for $s_x=0$, maximum value of the force F_{xM} and the value of the slip s_{xM}, the value of the force F_{xS} and the slip s_{xS}. The value of the F_x force depends on the vertical load degressively. Dependencies presented by Rill were utilised [7] for calculation of the values: $\left.\dfrac{dF_x}{ds_x}\right|_{(s_x=0)}$, F_{xM}, F_{xS}, s_{xM}, s_{xS}, for actual vertical wheel load. Referring to the longitudinal force F_{xM}, the dependence of F_{xM} on the vertical load is:

$$F_{xM}(F_z) = \frac{F_z}{F_N}\left[2F_{xM}(F_N) - \frac{F_{xM}(2F_N)}{2} - \left(F_{xM}(F_N) - \frac{F_{xM}(2F_N)}{2} \right)\frac{F_z}{F_N} \right],$$

$$s_{xM}(F_z) = s_{xM}(F_N) + \left(s_{xM}(2F_N) - s_{xM}(F_N) \right)\left(\frac{F_z}{F_N} - 1 \right),$$

(2)

F_N — nominal vertical tyre load,
$F_{xM}(F_N)$ — maximum value F_x for nominal load F_N,
$F_{xM}(2F_N)$ — maximum value F_x for load $2F_N$,
$s_{xM}(F_N)$ — value of the slip for F_{xM} for vertical load F_N,
$s_{xM}(2F_N)$ — value of the slip for F_{xM} for vertical load $2F_N$.

The remaining values: $\left.\dfrac{dF_x}{ds_x}\right|_{(s_x=0)}$, F_{xS}, s_{xS} were calculated similarly, by inserting functions of F_N and $2F_N$ into formula (2) (see [7], [9]).

The wheel – drum slip and wheel – roller slip were calculated as:

$$s = \frac{\omega_{ri}r_i - \omega_k r_{di}}{\omega_{ri}r_i},$$

(3)

ω_{ri}, r_i, ω_k, r_{di} — angular velocity and radii of the drum, support roller and wheel.

The initial values of the parameters for calculation $F_x(F_z,s)$ were taken from literature and then corrected on the basis of the performed experiment on the drum stand. The linear dependencies between the value of adhesion coefficient μ and values of the forces F_{xm}, F_{xS}, and slip s_{xM}, s_{xS} were assumed. The author's investigation showed that the slip point s_{xM} had bigger value on the drum stand

than that on the flat road surface. Value s_{xM} on the drum was in the range 30-50%. That conclusion was taken into consideration in the model of tyre – drum interaction on the stand.

The influence of the tyre circumferential stiffness was taken into consideration in the relationship representing moment of rolling resistance. The deformation of the tyre in circumferential direction under brake torque action shifts the radial reaction R and reduces the moment of rolling resistance [10]. It was assumed that during braking the shift of the reaction R is parallel to its previous direction. Moment of rolling resistance during braking was described as:

$$M_{ti} = R_i r_{di} f - R_i \Delta n_i , \qquad (4)$$

$$\Delta n_i = \frac{F_{ni}}{c_{op}} , \qquad (5)$$

Δn_i – deformation of the tyre in direction of F_{ni} force ($i = 1,2$),

c_{op} – circumferential stiffness of the tyre [N/m].

The radial stiffness of the tyre was determined on the roller of the stand. The tyre radial stiffness on the roller ($\phi = 0.25$ m) was about 10% lower than that on the flat surface.

The equations of motion in the stationary system (Oxz) are the following (denotations as in Fig. 2 and 3):

$$m_N \ddot{x}_N = (-F'_{x,p} - F'_{x,t})\cos\varphi_N + (F'_{z,p} + F'_{z,t})\sin\varphi_N ,$$

$$m_N \ddot{z}_N = (F'_{x,p} + F'_{x,t})\sin\varphi_N + (F'_{z,p} + F'_{z,t})\cos\varphi_N - G_N ,$$

$$I_N \ddot{\varphi}_N = -F'_{z,p}l'_p + F'_{z,t}l'_t + F'_{x,p}h'_p + F'_{x,t}h'_t + M_{hp} + M_{ht} ,$$

$$m_k \ddot{x}_{kp} = F'_{x,p}\cos\varphi_N - F'_{zp}\sin\varphi_N - F_{n2,p}\cos\alpha_{d2,p} -$$
$$- F_{n1,p}\cos\alpha_{d1,p} - R_{2p}\sin\alpha_{d2,p} + R_{1p}\sin\alpha_{d1,p} ,$$

$$m_k \ddot{z}_{kp} = -F'_{x,p}\sin\varphi_N - F'_{z,p}\cos\varphi_N - G_k + R_{2p}\cos\alpha_{d2,p} +$$
$$+ R_{1p}\cos\alpha_{d1,p} - F_{n2,p}\sin\alpha_{d2,p} + F_{n1,p}\sin\alpha_{d1,p} ,$$

$$m_k \ddot{x}_{kt} = F'_{x,t}\cos\varphi_N - F'_{z,t}\sin\varphi_N - F_{n2,t}\cos\alpha_{d2,t} - F_{n1,t}\cos\alpha_{d1,t}$$
$$- R_{2t}\sin\alpha_{d2,t} + R_{1t}\sin\alpha_{d1,t} ,$$

$$m_k \ddot{z}_{kt} = -F'_{x,t}\sin\varphi_N - F'_{z,t}\cos\varphi_N - G_k + R_{2t}\cos\alpha_{d2,t} +$$
$$+ R_{1t}\cos\alpha_{d1,t} - F_{n2,t}\sin\alpha_{d2,t} + F_{n1,t}\sin\alpha_{d1,t} ,$$

$$I_k \ddot{\varphi}_{kp} = F_{n1,p}r_{d1,p} + F_{n2,p}r_{d2,p} - M_{t1,p} - M_{t2,p} - M_{hp} - M_{opkp} ,$$

$$I_k \ddot{\varphi}_{kt} = F_{n1,t}r_{d1,t} + F_{n2,t}r_{d2,t} - M_{t1,t} - M_{t2,t} - M_{ht} - M_{opkt} ,$$

$$I_1 \ddot{\varphi}_{r1,p} = -F_{n1,p}r_1 - M_{t1,p} - M_{op1} ,$$

$$I_1 \ddot{\varphi}_{r1,t} = -F_{n1,t}r_1 - M_{t1,t} - M_{op1} ,$$

$$(I_{2,p} + I_{2,t})\ddot{\varphi}_{r2} = -(F_{n2,p} + F_{n2,t})r_2 - M_{t2,p} - M_{t2,t} - 2M_{op2} , \qquad (6)$$

Forces F_{ni}, R_i, G_k and moments M_h and M_t acting on the wheel are shown in Fig. 3. Moments M_{opkp}, M_{opkt} in equation (6) are the moments of the wheels ventilation and wheels bearings resistance. M_{op1} and M_{op2} represent moments of bearing resistance of the roller I_1 and drum I_2. Forces F'_x and F'_z acting on the car body in the x' and z' directions are calculated as:

$$F'_{x,p} = \Delta x'_p c_{xp} + \Delta \dot{x}'_p k_{xp},$$
$$F'_{x,t} = \Delta x'_t c_{xt} + \Delta \dot{x}'_t k_{xt},$$
$$F'_{z,p} = \Delta z'_p c_{zp} + \Delta \dot{z}'_p k_{xp} + F_{z,p0}, \tag{7}$$
$$F'_{z,t} = \Delta z'_t c_{zt} + \Delta \dot{z}'_t k_{xt} + F_{z,t0},$$
$$F_{z,p0} = G_N \frac{l_t}{l}, F_{z,t0} = G_N \frac{l_p}{l}.$$

The suspensions deformations in the x' and z' directions are (Fig. 2b):

$$\Delta x'_i = l_i - l'_i,$$
$$\Delta z'_i = h_N - h'_{Ni}, \quad i = p,t \tag{8}$$

l_i, h_N – distances between centre of the car body mass and axle of the front and rear wheels, and height of centre of mass over the axle of the wheels in the static equilibrium.

Parameters l_i and h_N were determinated experimentally.

The distances l'_i and h'_{Ni} were calculated from:

$$l'_i = \left| (x_{ki} - x_N) \cos \varphi_N - (z_{ki} - z_N) \sin \varphi_N \right|,$$
$$h'_{Ni} = \left| (x_{ki} - x_N) \sin \varphi_N + (z_{ki} - z_N) \cos \varphi_N \right|, \quad i = p,t. \tag{9}$$

The remaining forces and moments acting on the system were calculated from:

$$R_{1i} = (r_{sw} - r_{d1i})c_r - \dot{r}_{d1i} k_{op}, \qquad R_{2i} = (r_{sw} - r_{d2i})c_r - \dot{r}_{d2i} k_{op},$$
$$F_{n1i} = F(R_{1i}, s_{1i}, \mu), \qquad F_{n2i} = F(R_{2i}, s_{2i}, \mu), \tag{10}$$
$$M_{t1i} = M(R_{1i}, r_{d1i}, f(\omega_{ki}), \Delta n_i), \quad M_{t2i} = M(R_{2i}, r_{d2i}, f(\omega_{ki}), \Delta n_i), \quad i = p,t.$$

The equations of motion (6) contain dynamic radii r_{d2}, r_{d1} and angles α_{d1}, α_{d2}. For the pneumatic wheels, the radii and the angles change their values during braking. The values of the radii r_{d2}, r_{d1} and angles α_{d1}, α_{d2} were determined from the geometric dependencies on the basis of Fig. 5:

$$(r_1 + r_{sw}) \sin \alpha_1 = (r_{d1} + r_1) \sin \alpha_{d1} - \Delta x_k,$$
$$(r_1 + r_{sw}) \cos \alpha_1 = (r_{d1} + r_1) \cos \alpha_{d1} - \Delta z_k, \tag{11}$$

r_{sw} – free radius of the wheel (unloaded wheel),
$\Delta x_k, \Delta z_k$ – displacement of the wheel centre during braking, $\Delta x_k < 0, \Delta z_k < 0$.
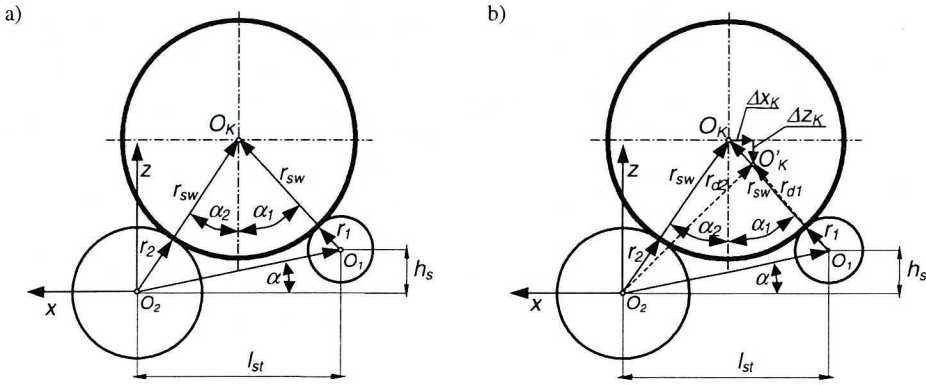
Fig. 5. Position of the wheel on the rollers of the stand. a) without forces acting between wheel and rollers, b) displacement of the centre of the wheel Δx_k, Δz_k during braking

By solving the system of the equations (11), we can determine dynamic radius r_{d1} and angle α_{d1}:

$$r_{d1} = \sqrt{(r_1 + r_{sw})^2 + 2(r_1 + r_{sw})(\Delta x_k \sin\alpha_1 + \Delta z_k \cos\alpha_1) + \Delta x_k{}^2 + \Delta z_k{}^2} - r_1,$$

$$\alpha_{d1} = \arcsin\left(\frac{(r_1 + r_{sw})\sin\alpha_1 + \Delta x_k}{r_{d1} + r_1}\right). \tag{12}$$

In the same way we can determine dynamic radius r_{d2} and angle α_{d2}:

$$r_{d2} = \sqrt{(r_2 + r_{sw})^2 + 2(r_2 + r_{sw})(-\Delta x_k \sin\alpha_2 + \Delta z_k \cos\alpha_2) + \Delta x_k{}^2 + \Delta z_k{}^2} - r_2,$$

$$\alpha_{d2} = \arcsin\left(\frac{(r_2 + r_{sw})\sin\alpha_2 + \Delta x_k}{r_{d2} + r_2}\right). \tag{13}$$

On the basis of the Fig. 5a we can calculate The angles α_1 and α_2 for free radius r_{sw}:

$$l_{st} - (r_1 + r_{sw})\sin\alpha_1 = (r_2 + r_{sw})\sin\alpha_2,$$

$$h_{st} + (r_1 + r_{sw})\cos\alpha_1 = (r_2 + r_{sw})\cos\alpha_2. \tag{14}$$

The solution to the system (14) is:

$$a_i = 2\arctan\left(\frac{A_i \pm \sqrt{A_i{}^2 + B_i{}^2 - C_i{}^2}}{B_i + C_i}\right), \quad i = 1, 2,$$

$$A_i = -2l_{st}(r_i + r_{sw}),$$

$$B_i = 2h_{st}(r_i + r_{sw}), \tag{15}$$

$$C_1 = (r_2 + r_{sw})^2 - (r_1 + r_{sw})^2 - (h_{st}{}^2 + l_{st}{}^2),$$

$$C_2 = (r_1 + r_{sw})^2 - (r_2 + r_{sw})^2 - (h_{st}{}^2 + l_{st}{}^2).$$

The dependencies of dynamic radii and angles were used in braking simulations on the stand.

The brake moments of the front and rear wheels measured during ABS operation were assumed as the input functions (Fig. 6). More details about the control algorithm of the ABS system are presented in p. 4.

The response of the system to this input functions, in the range of ABS frequencies, was analysed. The additional inputs, for example connected with shape deviation or wheels unbalance were disregarded. The initial conditions are the following:

$$x_N(0) = x_{N0}, \quad z_N(0) = z_{N0}, \quad \varphi_N(0) = \varphi_0, \quad \dot{x}_N(0) = 0, \quad \dot{z}_N(0) = 0, \quad \varphi_N(0) = 0;$$

$$x_{k,i}(0) = x_{ki,0}, z_{k,i}(0) = z_{ki,0}, \dot{x}_{k,i}(0) = 0, \quad z_{k,i}(0) = 0, \quad \varphi_{k,i}(0) = 0, \dot{\varphi}_{k,i}(0) = \omega_{0k,i};$$

$$\varphi_{r1i}(0) = 0, \quad \dot{\varphi}_{r1i}(0) = \omega_{r1i,0};$$

$$\varphi_{r2}(0) = 0, \quad \dot{\varphi}_{r2}(0) = \omega_{r2,0}.$$

(16)

Values z_{N0} and z_{k0} result from static deflections of the suspension and tyre. Value $\omega_{r2,0}$ is the initial angular velocity of the stand drums 2 (Fig. 2). Values $\omega_{r1,0}$ (rollers) and $\omega_{ki,0}$ (wheels) result from the angular velocity $\omega_{r2,0}$ of the drums 2 and from values of the wheel radii r_{di} on the rollers at the initial time moment.

Numerical solution to the differential equations (6) can be obtained by reduction of the second order equations to the first order. The following replacement was applied:

$$[y_1 y_2 y_3 y_4 y_5 y_6 y_7 y_8 y_9 y_{10} y_{11} y_{12}]^T = [x_N z_N \varphi_N x_{kp} z_{kp} x_{kt} z_{kt} \varphi_{kp} \varphi_{kt} \varphi_{r1p} \varphi_{r1t} \varphi_{r2}]^T,$$

$$[y_{13} y_{14} y_{15} y_{16} y_{17} y_{18} y_{19} y_{20} y_{21} y_{22} y_{23} y_{24}]^T = [\dot{x}_N \dot{z}_N \dot{\varphi}_N \dot{x}_{kp} \dot{z}_{kp} \dot{x}_{kt} \dot{z}_{kt} \dot{\varphi}_{kp} \dot{\varphi}_{kt} \dot{\varphi}_{r1p} \dot{\varphi}_{r1t} \dot{\varphi}_{r2}]^T.$$

For that replacement, the equations (6) have the form:

$$\frac{d}{dt}[y] = \begin{bmatrix} y_{13} \\ \vdots \\ y_{24} \\ \dfrac{1}{m_N}[(-F'_{x,p} - F'_{x,t})\cos\varphi_N + (F'_{z,p} + F'_{z,t})\sin\varphi_N] \\ . \\ . \\ . \\ \dfrac{1}{(I_{2,p} + I_{2,t})}[-(F_{n2,p} + F_{n2,t})r_2 - M_{t2,p} - M_{t2,t} - 2M_{op2}] \end{bmatrix}$$

(17)

The system of 24 differential equations (first order) was obtained. The program „ode45" in Matlab 6.0 was applied to solve the system numerically [11]. In the result, the time functions of the generalised co-ordinates and their derivatives were obtained:

$$[x_N z_N \varphi_N x_{k,i} z_{k,i} \varphi_{k,i} \varphi_{r1i} \varphi_{r2}], [\dot{x}_N \dot{z}_N \dot{\varphi}_N \dot{x}_{k,i} \dot{z}_{k,i} \dot{\varphi}_{k,i} \dot{\varphi}_{r1i} \dot{\varphi}_{r2}].$$

3.1. Results of simulation

The results of the calculations were verified against the results of experimental investigation. Examples of simulation and experiments are shown in Fig. 7–16. The comparison of these results showed that the changes and values of the wheel and drum speed were similar in the simulation and experimental investigation of vehicle (passenger car middle class). The model of braking on the stand with
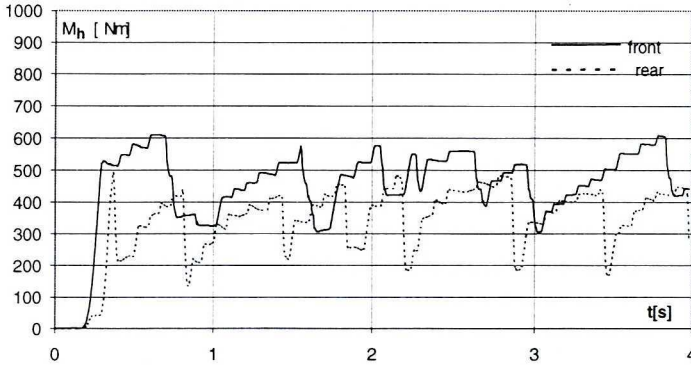

Fig. 6. Brake moments for front and rear wheels during ABS acting. Results of the stand experimental investigation
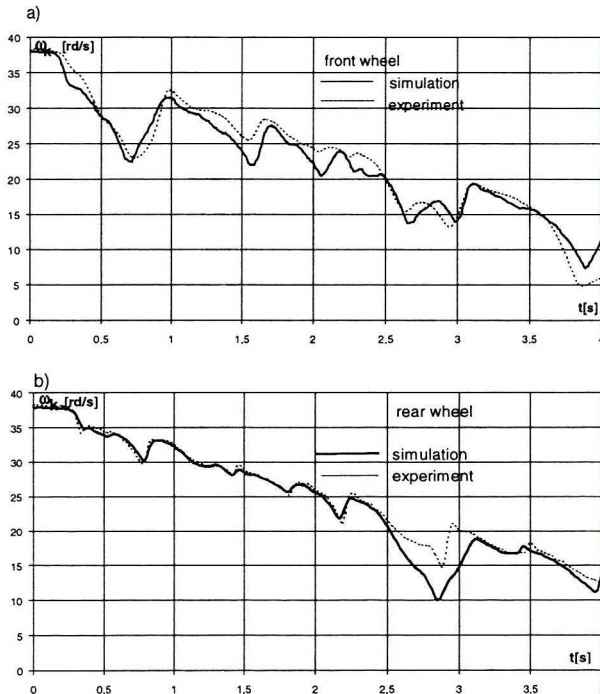
Fig. 7. Changes of the angular velocities of the wheels during braking under brake moments M_h shown in Fig. 6. a) front wheel, b) rear wheel

flywheels gave the results consistent with the results of investigation. The results of simulations showed that all significant parameters of the vehicle and stand were taken into account.
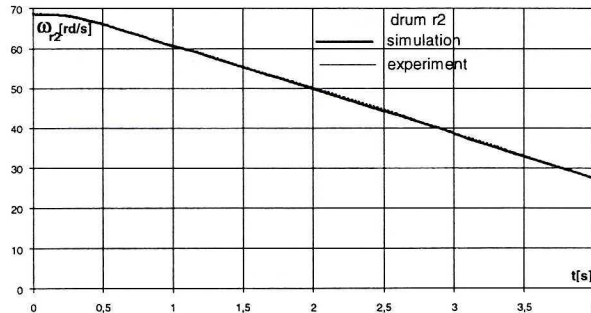
Fig. 8. Changes of the angular velocity of the drums of the stand during braking under brake moments M_h shown in Fig. 6

The influence of the suspensions and tyres stiffness and damping on the vibration and angular velocity of the wheels is shown in Fig. 9–11. The amplitude of the centre of wheel vibration is about 0.008 m. Changes of longitudinal and vertical stiffness of the suspension and changes of the tyres damping have small influence on the angular velocity of the wheels (Fig. 12, 13).
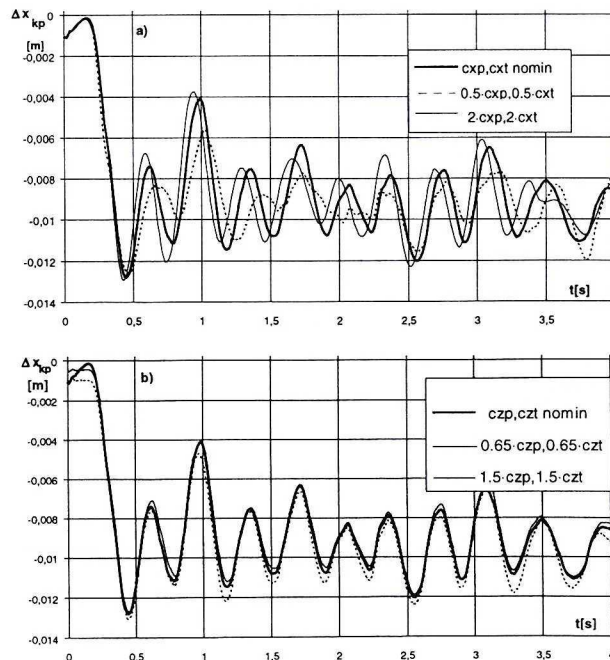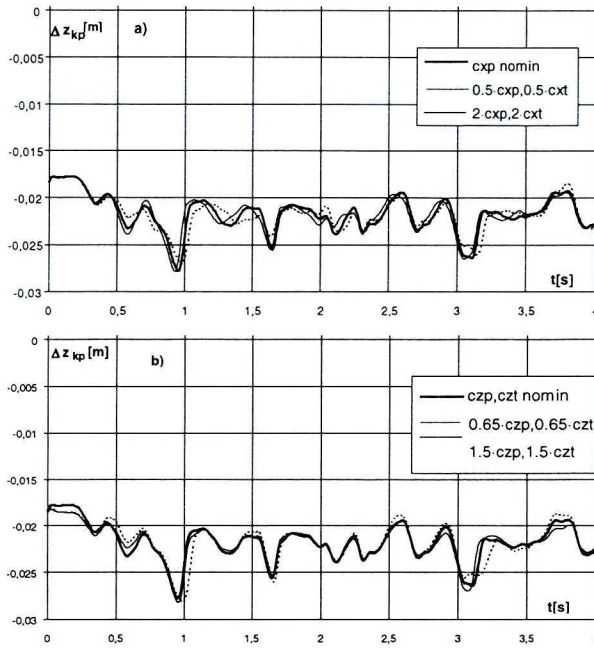

Fig. 9. Influence of the longitudinal (a) and vertical (b) stiffness of the suspension on the centre of wheel displacement in x direction during braking on the stand with ABS acting. Nominal values:
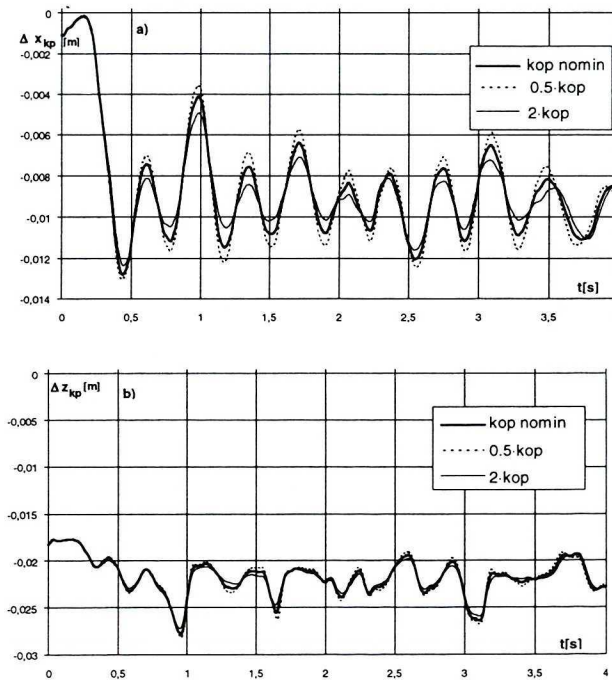c_{xp} = 265 kN/m, c_{xt} = 365 kN/m, c_{zp} = 21 kN/m, c_{zt} = 28 kN/m

Fig. 10. Influence of the longitudinal (a) and vertical (b) stiffness of the suspension on the centre of wheel displacement in z direction during braking on the stand with ABS acting

Fig. 11. Influence of the tyre damping on the centre of wheel displacement in x (a) and z (b) direction during braking on the stand with ABS acting. $k_{op}=100$ Ns/m
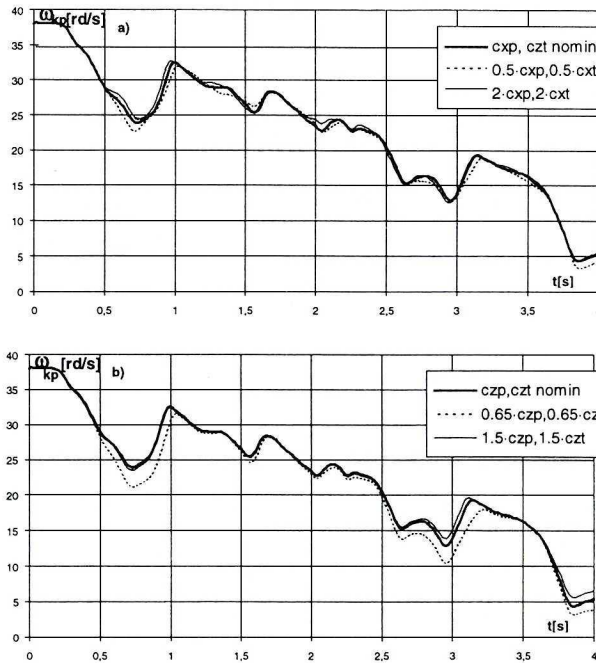
Fig. 12. Influence of the longitudinal (a) and vertical (b) stiffness of the suspension on the angular velocity of the front wheel during braking on the stand with ABS acting
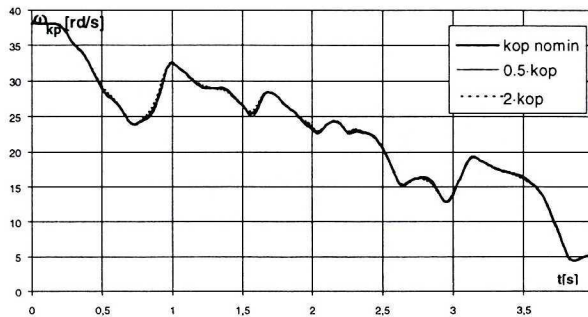

Fig. 13. Influence of the tyre damping on the angular velocity of the front wheel during braking on the stand with ABS acting. k_{op}=100 Ns/m

One noticed the influence of the tyre radial stiffness on vibration and angular velocity of the wheel (Fig. 14, 15). Amplitude of vibrations of the centre of wheel increased when radial stiffness of the tyre c_r decreased. Angular body vibrations appeared during tests of the ABS system. Angular velocity of the body about the y axis was measured by gyroscope and compared with the results of the simulations (Fig. 16). Amplitude of angular velocity ω_{yN} had greater values in simulations than in the tests on the stand. Frequency of the vibration was the same in the tests as and the simulations.
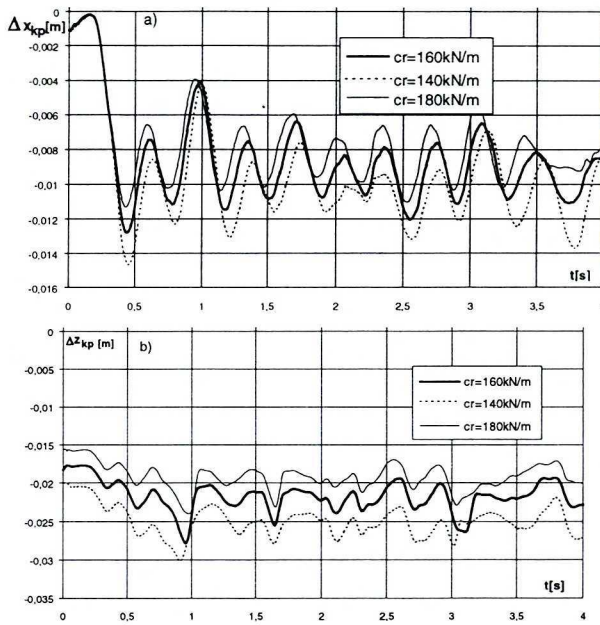
Fig. 14. Influence of the tyre radial stiffness on the wheel displacement in x (a) and z (b) direction during braking on the stand with ABS acting
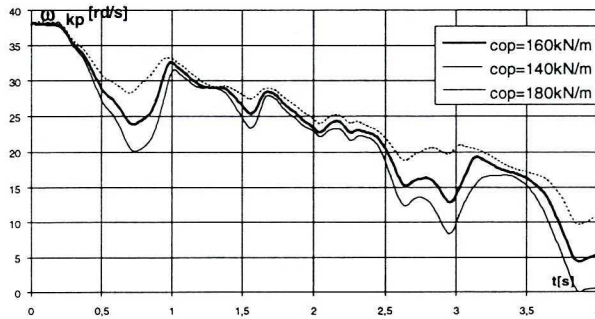

Fig. 15. Influence of the tyre radial stiffness c_{op} on the angular velocity of the front wheel during braking on the stand with ABS acting
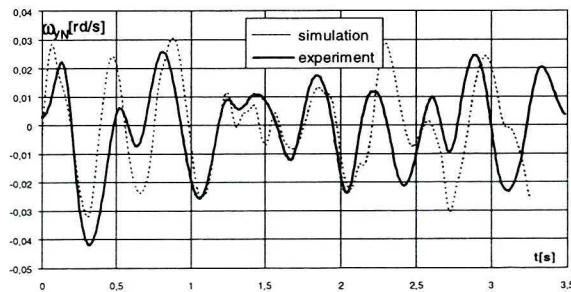

Fig. 16. Angular velocity of the vehicle body during braking on the stand with ABS acting. Results of simulation and experimental investigation

Characteristic of the longitudinal force versus wheel slip $F_n(s_x)$ had an influence on the angular velocity of the wheels during braking with ABS operating (Fig. 17). Stand investigation of the tyres showed that the maximum value of the coefficient of longitudinal adhesion utilization occurs at a higher value of the slip than in road conditions. The value s_{xM} on the stand was in the range 30–50%. The results of simulations were closed to the results of experiments on the stand when the s_{xM} point was greater than 20%.

The results of the simulations showed that suspension and tyre parameters (stiffness and damping) exerted an influence on the wheel vibrations and on the velocity of the wheel during ABS operation. The vibrations did not disturb the diagnostic tests of brakes.
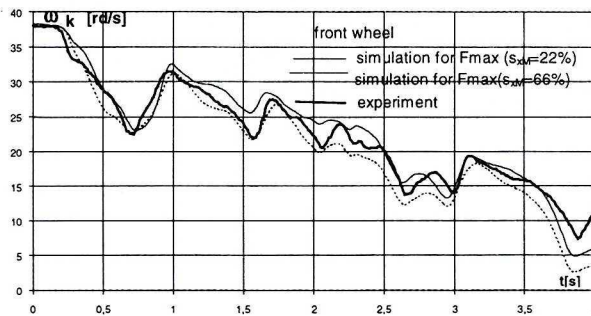

Fig. 17. Influence of the tyre characteristic $F_x(s)$ on the angular velocity of the front wheel during braking on the stand with ABS acting

4. Results of ABS investigation on the drum stand

The investigation on brakes with ABS system was carried out on the drum stand (Fig. 1). The results of the tests are shown in Fig. 18–20. The peripheral speed of drums v_s (matching car speed), wheels speed v_k and wheels slip s at the time of intensive braking with ABS acting are presented. Slip of the braked wheels was calculated directly after tests. These dependencies correspond to a car braking on the road with constant and changing tyre to road coefficient of adhesion, during straight ahead braking.

A qualitative assessment of ABS operation can be made on the basis of these diagrams It consists of:

- Estimation of the lock duration of the braked wheels and the frequency of regulation. According to [8], momentary locks are permissible, which don't cause any loss of stability and steerability of the car. For the tested ABS, the lock moments did not occur for the vehicle speed above 5 km/h.
- Estimation of the lowest speed of ABS operation. The tested ABS switched off the operation when the wheel speed reached about 5 km/h and the car wheels stopped with blocking.

— Estimation of ABS operation on a homogeneous surface of the stand by comparison of the courses of speeds for left and right wheels, Fig. 18.

— Estimation of ABS adaptation to changing conditions of adhesion between wheel and drum surface (*μ-sprung* surface). This effect was obtained by sudden wetting of the dry surface of drum. This test made it possible to check the response of ABS to the jump input.

— Estimation of ABS adaptation to braking on the *μ-split* surface. We could observe individual regulation for front wheels and select low regulation for rear wheels on that kind of surface.
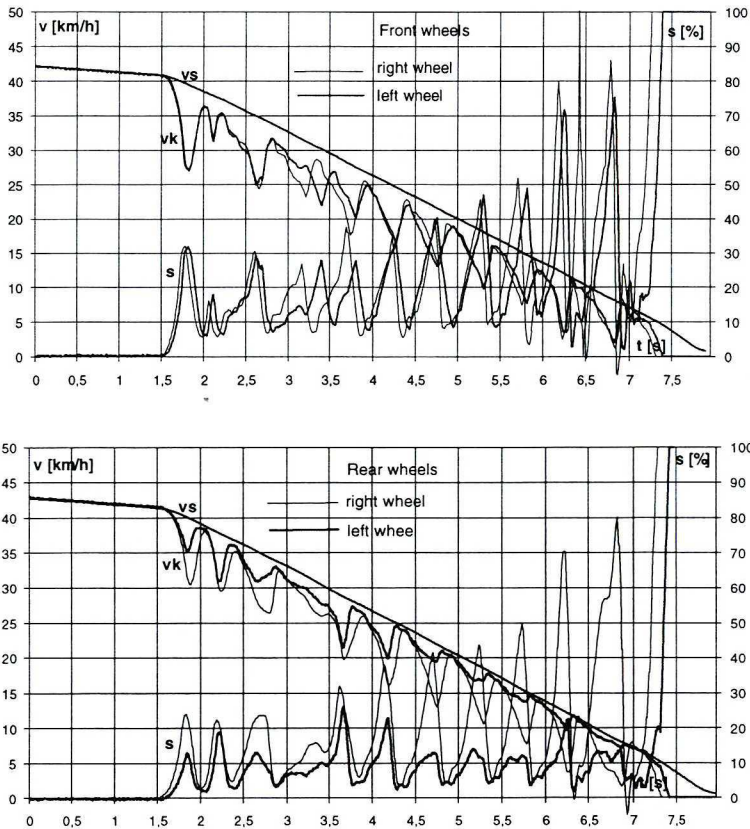

Fig. 18. Changes of the speed of drums v_s (matching vehicle speed), wheels speed v_k and slip s during braking with ABS operating on dry, homogeneous surface of the stand

Changes of the wheel speed and slip of right and left rear wheels were observed during braking on the *μ-split* surface (Fig. 20). The ABS controller controlled the motion of the rear wheels using the *select low* principle. The deceleration and slip of the rear wheels were controlled on the basis of the parameters for wheel which ran on the more slippery surface. It caused that wheel which ran on the surface with high adhesion coefficient had smaller

changes of the speed and smaller slip than opposite wheel on the surface with
low adhesion coefficient. The graphs in Fig. 20 show that the rear left wheel
was braked on the more slippery surface and the rear right wheel on the surface
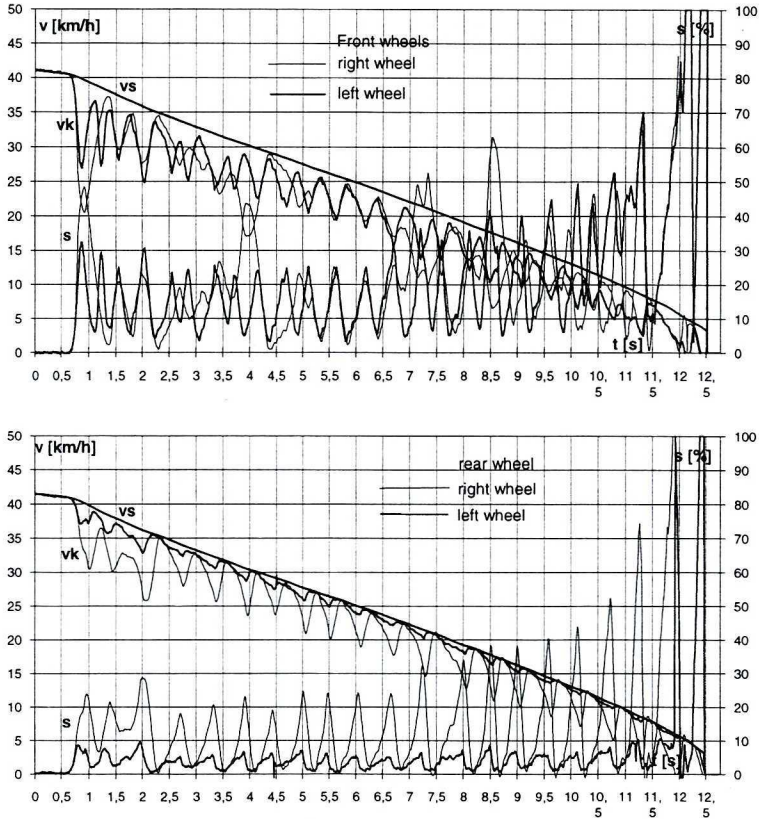with higher adhesion coefficient.

Fig. 19. Changes of the speed of drums v_s (matching vehicle speed), wheels speed v_k and slip s
during braking with ABS operating on wet surface of the stand

The differences in the speed and slip changes for rear wheels could be
caused not only by the changes of adhesion coefficient but also by the changes
of the wheel vertical load. The tangential force between wheel and road depends
on the adhesion coefficient as well as on vertical load of the wheel. At *select
low* principle of the ABS operation, the same changes of brake moments for
right and left wheel can cause different motion of these wheels if their normal
loads are not equal. The wheel with smaller vertical load reaches the limit value
of the deceleration and slip earlier. The wheel which is more loaded reaches the
limit values later. As the result, we can observe asymmetric action of ABS
under *select low* operation on the homogenous surface (different velocity
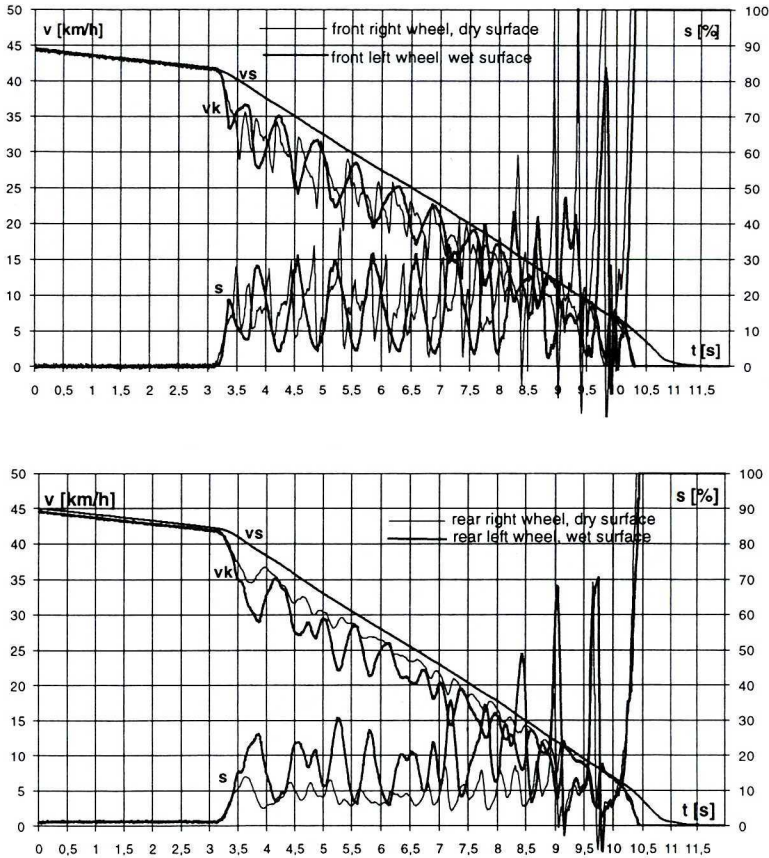amplitude and slip of the rear wheels).

Fig. 20. Changes of the speed of drums v_s (matching vehicle speed), wheels speed v_k and slip s during braking with ABS operating on μ-split surface of the stand

The results of investigation confirmed that *select low* principle limited adhesion utilization not only on the μ-split surface, but also on the homogenous surface under asymmetric vertical load of the right and left side of the vehicle.

The stand investigation made it possible to estimate control algorithm of ABS control unit. We could analyse cycles of ABS action in different conditions of adhesion coefficient. The results of investigation are presented in Fig. 21, 22. The pressure in the front brake calliper, speed of the car v_s, speed of the wheel v_k were measured. The circumferential deceleration and slip of the wheels were calculated. In the tested ABS brake system, the stopping of the pressure increase was observed when deceleration of the wheel reached the value of 15...20 m/s². The pressure intensively decreased when slip of the wheel reached the value of about 20–25%. When the wheel passed from deceleration to acceleration motion, the drop of the pressure was stopped to the moment when the wheel slip decreased bellow the boundary value. From this moment,

the pressure increased again (step by step). The speed of the pressure decrease
and increase was different in order to avoid excitation of the axles resonance
[1].

The analysis of the pressure time functions enables us to estimate differences
between the algorithms of the pressure control by ABS control unit, on the road
with high and low adhesion coefficient (on dry and wet surface). On the high
grip road surface the single drop (impulse) of the pressure was sufficient to put
the wheel into acceleration motion. On the slippery road the pressure dropped in
a few impulses, because the time to the put the wheel into acceleration motion
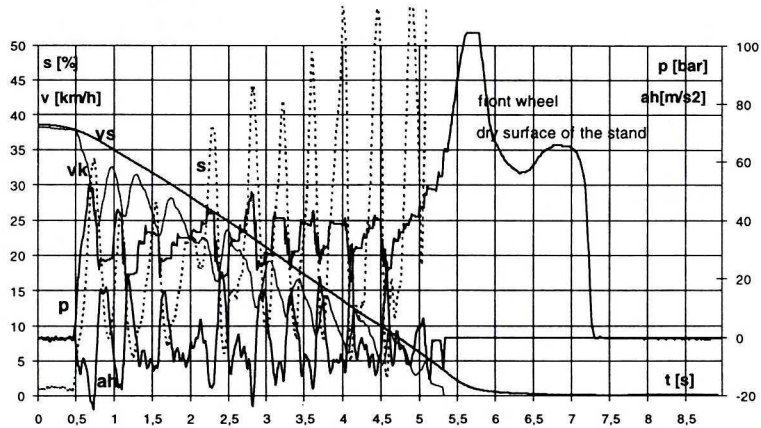was longer.

Fig. 21. Changes of the speed of drums v_x (matching vehicle speed), wheels speed v_k and slip s,
peripheral wheel deceleration a_h and pressure in brake calliper p during braking with ABS on dry
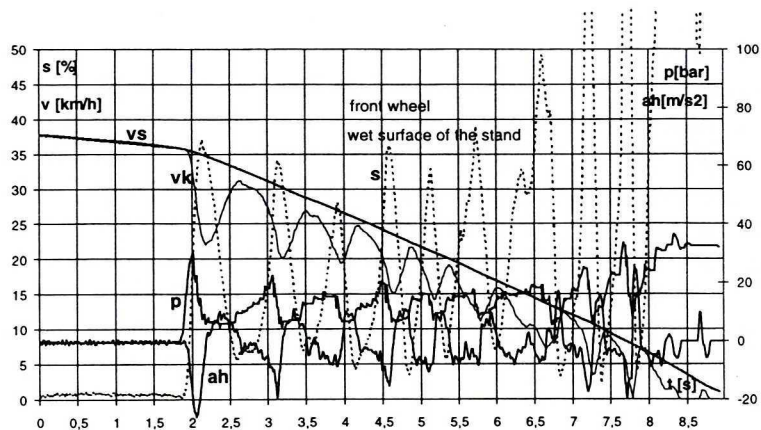surface of the stand

Fig. 22. Changes of the speed of drums v_x (matching vehicle speed), wheels speed v_k and slip s,
peripheral wheel deceleration a_h and pressure in brake calliper p during braking
with ABS on wet surface of the stand

The differences in the length of the time of pressure increase were observed too. On the wet surface of the drums, the time of the pressure increase was longer than on the dry surface.

These differences between the algorithms on the surfaces with high and low coefficient of adhesion result from the wheels behaviour in the braking and acceleration phase of transition. The time from the deceleration to acceleration motion of the wheel depended on the tyre - drum coefficient of adhesion. If the coefficient of adhesion was low, the time of the wheel transition from deceleration to acceleration motion became longer. In that phase of wheel motion, the derivative da_h/dt decreased on the surface with low coefficient of adhesion.

The parameter da_h/dt or the time of the pressure reduction in the brake calliper can be used for current, rough estimation of the road coefficient of adhesion and for a choice of ABS algorithm for current state of road surface.

The quantitative analysis of ABS operation were performed on the basis of the results of measurements on the stand:
– estimation of the wheel slip regulation,
– estimation of adhesion utilization,
– estimation of symmetry of ABS operation on the homogeneous surface by frequency response functions of wheels deceleration or wheels slip,
– statistical analysis of ABS operation (probability distribution of wheel slip $P(s_i)$).

These quantitative parameters are presented in [2], [3], [4], [5].

5. Comparison of the results of experimental investigation in stand and road conditions

The stand and road investigation were carried out with the same measurement equipment. The rotational velocities of the wheels on the stand and on the road were measured using the same sets of the digital sensors mounted to the wheels. The circumferential speed of the drums of the stand and speed of the car on the road were measured by optical system Correvit.

The results of the tests showed the differences between time functions of the wheel speed in the stand and road conditions (Fig. 23, 24). It pertained to the amplitude and frequency of the wheels speed during braking with ABS acting. These differences could result from the conditions of mating between wheels and drums of the stand or between wheels and flat surface of the road. In the stand conditions, the moment of inertia of the support roller (1 in Fig. 2) influenced the changes of wheel speed during braking. The influence was similar to increasing the moment of inertia of the wheel. When the moment of inertia of the wheel increased, the limit value of the circumferential wheel deceleration could be reached at the greater value of the wheel slip. Then, it was possible that on the stand the amplitude of the wheel speed and slip was greater

than on the road. Besides, there were differences between coefficient of adhesion in stand and road investigation.

These differences don't disqualify diagnostic method of ABS evaluation on the drum stand. Because of the differences in stand and road conditions, the criteria for the ABS evaluation should be established in stand conditions.
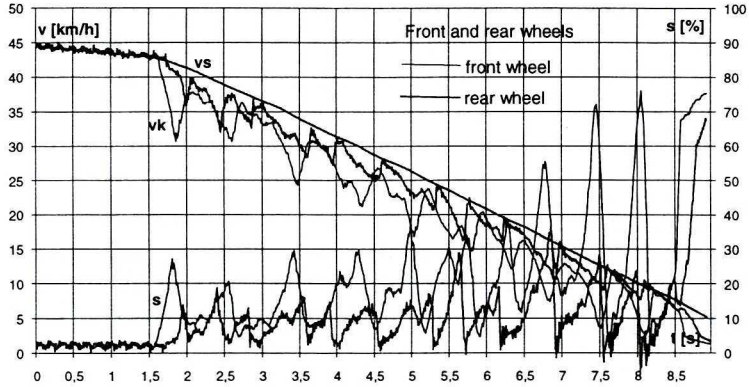

Fig. 23. Changes of the speed of drums v_s (matching vehicle speed), front wheels speed v_k and slip s during braking with ABS acting on the stand
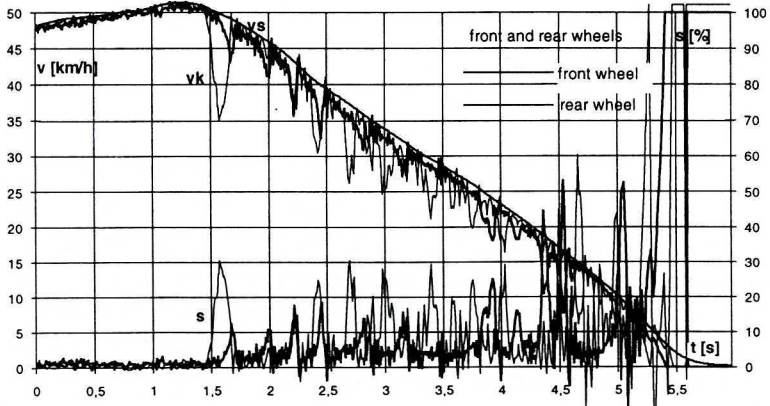

Fig. 24. Changes of the vehicle speed v_s, front wheels speed v_k and slip s, during braking with ABS acting on the road. Wet asphalt

6. Conclusions

1. Model of the vehicle – drum stand system makes it possible to evaluate the influence of the suspension and tyre parameters on the vehicle vibrations and angular velocities of wheels during braking with ABS acting. The vibrations of the wheels and the body don't disturb the diagnostic tests of the brake system.

2. The presented method of ABS diagnostic tests in stand conditions facilitates examination of the antilock units regardless of the mechanical design, electronic systems and program versions. The criteria of evaluation are versatile for all kinds of ABS systems.

3. The stand construction makes it possible to test the ABS systems in changing conditions of adhesion utilization. The stand construction makes it possible to change front and rear drums base to the wheel base of the tested vehicle.

4. The results of the tests showed the differences between the wheel speed time functions during ABS action in the stand and road conditions.

5. Establishing the limit values of diagnostic parameters for evaluation of ABS operation requires consultations with producers of antilock units.

REFERENCES

[1]   Antilock Braking System ABS. Technical Information. Bosch Gmbh, 1993.

[2]   Gajek A.: Estimation of ABS operation in stand conditions. Brake Conference 97', Institute of Vehicles, University of Technology, Łódź 09/1997.

[3]   Gajek A.: Testing of ABS operation in stand conditions. International Conference BRAKES 2000, The University of Leeds, The Institution of Mechanical Engineers (IMechE). Leeds, UK 07/2000.

[4]   Gajek A.: Analiza działania układu ABS w warunkach stanowiskowych. Teka Komisji Naukowo-Problemowej Motoryzacji, PAN Oddział w Krakowie, Zeszyt 20, Kraków, 2000.

[5]   Gajek A.: Modelowanie i analiza układu samochód – stanowisko bębnowe do badań i diagnostyki hamulców. Monografia nr 280, Politechnika Krakowska, Kraków 2002.

[6]   Durski B.: Analytic expression of dependencies between coefficient of adhesion, wheel slip and speed of the vehicle. Brake Conference 88', Institute of Vehicles, University of Technology, Łódź 09/1988.

[7]   Hirschberg W., Rill G., Weinfurter H.: User-Appropriate Tyre-Modelling for Vehicle Dynamics in Standard and Limit Situations. Vehicle System Dynamics, 2002, vol. 38, No 2, pp. 103÷125.

[8]   Regulations NR 13 ECE, Ann. NR 13: Requirements for investigation of brakes equipped with ABS systems.

[9]   Rill G.: Simulation von Kraftfahrzeugen. Vieweg & Sohn Verlagsgesellschasft, Braunschweig/Wiesbaden 1994.

[10]   Szczepaniak C., Lanzendoerfer J.: Teoria ruchu samochodu. WKŁ, Warszawa 1980.

[11]   Zalewski A., Cegieła R.: Matlab – Obliczenia numeryczne i ich zastosowania. Wyd. Nakom. Poznań 1997.

Ocena działania układu przeciwblokującego ABS w warunkach stanowiskowych

Streszczenie

Szerokie zastosowanie układów przeciwblokujących w hamulcach pojazdów samochodowych powoduje konieczność ich kontroli w okresie eksploatacji samochodu. Obecnie kontrola ta obejmuje diagnozowanie elementów elektrycznych i elektronicznych poprzez system autodiagnostyki zintegrowany z jednostką sterującą ABS. W pracy podjęto problem diagnozowania układów przeciwblokujących jako całości, w warunkach stanowiskowych. Zaproponowano koncepcję kontroli działania układu ABS na stanowisku bębnowym z masami wirującymi. Opracowano model układu samochód–stanowisko diagnostyczne i przeanalizowano wpływ wymuszenia zmiennymi momentami hamującymi kół przednich i tylnych na drgania pojazdu na stanowisku. Zaproponowano zasady oceny stanu układu przeciwblokującego w tej metodzie diagnostycznej poprzez pomiar prędkości kół pojazdu poddanych działaniu układu ABS. Przedstawiono jakościowe wskaźniki oceny działania układu ABS. Wyniki analiz teoretycznych zweryfikowano wykonując badania samochodów z układami ABS na prototypowym stanowisku bębnowym. Rezultaty badań pozwoliły na opracowanie metody stanowiskowej kontroli układu hamulcowego z układem przeciwblokującym.